Voronoi analysis of the breakdown of order in spontaneous optical spot patterns

G. Schliecker and R. Neubecker*

Max-Planck-Institut für Physik Komplexer Systeme, Nöthnitzer Straße 38, 01187 Dresden, Germany

(Received 25 October 1999)

In a nonlinear optical single feedback system, patterns of bright spots evolve spontaneously. Making use of the Voronoi construction, the breakdown of spatial order in experimental spot patterns under increase of the pump laser intensity is analyzed. The spot density is found to increase with the pump intensity. Our analysis shows that maximum order is maintained for a finite range of spot densities and starts to break down at a clearly detectable threshold value. The enhanced disorder with increasing density contrasts the behavior of simple hard-core systems. A separate analysis of the metrical properties of the Voronoi cells in ordered and disordered regions yields remarkably smaller nearest-neighbor distances in disordered regions. This suggests that the creation of new spots is a governing mechanism for the observed breakdown of order.

PACS number(s): 05.65.+b, 64.70.Dv, 42.65.Sf, 68.90.+g

The spontaneous evolution of spatiotemporal structures as in heated layers of liquids, oscillating spirals in chemical reactions, or the onset of turbulence in flows can in principle appear in any extended, open and nonlinear system [1]. A large number of systems follow a typical scenario with at least two instabilities: under an increase of the external control parameter, commonly the power flow through the system, from a steady and uniform state first well-ordered, stationary and spatially periodic patterns evolve spontaneously. Then, under further increase of the control parameter, spatial order breaks down and the structures become dynamic.

While there are mathematical tools to treat these systems close to the first threshold [1], far above the threshold in the complex, dynamic regime no analytic approaches exist. In this region, a quantitative analysis of the states can be performed only by means of empirical and statistical methods. The methods of stochastic geometry are known to form a reliable and efficient tool for the characterization of order-disorder transitions in various planar systems [2,3]. Here, we apply for the first time the Voronoi construction to spot patterns in a nonlinear optical system, in order to gain a deeper insight into evolution of disorder and the properties of the states in the complex, dynamic regime.

The optical system under consideration belongs to the class of the *single-feedback* systems [4]. In such setups, a uniform pump laser beam with a broad cross section is modulated by a nonlinear medium, freely propagates through a feedback loop and is then fed back to the nonlinear medium. The combination of nonlinearity and diffractional spatial coupling, resulting from the propagation, leads to a modulational instability. As consequence, spatial patterns emerge in the transverse cross section of the light beam.

In our case, a saturable Kerr-type nonlinearity is provided by a liquid crystal light valve (LCLV), which allows one to observe large aspect-ratio patterns [5–7]. The LCLV is a multilayer device with a phase-modulating reflective read-out and an absorptive write side. The spatial read-out phase profile is determined by the light intensity distribution at the write side of the LCLV.

Figure 1 shows a simplified diagram of the experimental setup. A laser beam is phase-modulated and reflected by the LCLV read-out side and then fed back to the LCLV write side, after propagation over the length L. In the experiment, the intensity distribution at the LCLV write side is recorded. Above a threshold intensity of $I_p \approx 50\ \mu\mathrm{W/cm}^2$, the initially uniform cross section of the beam breaks up into patterns of bright spots, typically in a hexagonal arrangement.

The theoretical description of the system [7] is based on two coupled partial differential equations. A quantitative relation between the induced phase shift of the reflected beam $\Phi(x,y,t)$ and the modulating intensity $I_w(x,y,t)$ at the write side of the LCLV is given by

$$\tau\dot{\Phi} - l^2\nabla_\perp^2\Phi + \Phi = \frac{\Phi_{max}}{\cosh^2\left(\dfrac{1+\kappa_r I_w}{1+\kappa_s I_w}\hat{V}_{ext} - \hat{V}_{th}\right)}, \qquad (1)$$

with the transversal spatial coordinates x and y and the time t. The temporal response and the spatial coupling within the LCLV are included in lowest order with a relaxation time $\tau \approx 50$ ms and an effective diffusion length $l \approx 30\ \mu$m. In our system, diffusional spatial coupling does not cause the spatial instability. The right-hand side of Eq. (1) describes the nonlinear, saturable response of the induced phase on the

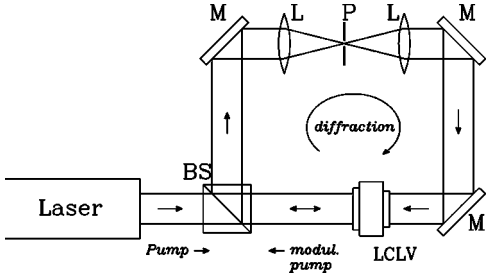

FIG. 1. Schematic diagram of the setup: the expanded laser beam is reflected at the LCLV read-out side, thereby acquiring a phase shift profile and is then fed back to the write side with the beam splitter (BS) and the mirrors M. A spatial low-pass filter (lenses L, aperture P) restricts the active wave numbers to the lowest unstable band.

*Present address: Institut für Angewandte Physik, Hochschulstr. 6, 64289 Darmstadt, Germany.

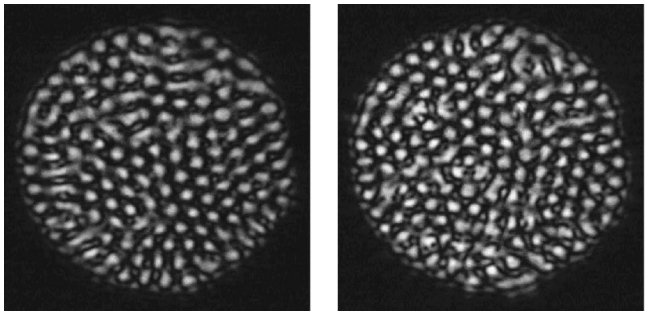

FIG. 2. Snapshots of the experimental intensity distribution at the LCLV for $I_{rel}=3.6$ (lhs) and $I_{rel}=5.16$ (rhs). The typical diameter of such a pattern is 6 mm.

write intensity I_w. $\hat{V}_{ext}$ is the scaled external supply voltage of the LCLV, $\hat{V}_{th}$ describes an internal threshold, and κ_r, κ_s are device specific parameters. Here, we are concerned with a nonlinearity of self-focusing type ($d\Phi/dI_w>0$) only [7,9].

Due to the propagation, the spatial modulation of the phase shift is transformed to the intensity profile at the write side of the LCLV,

$$I_w=|\exp[-i(L/2k_0)\nabla_\perp^2]\exp(-i\Phi)|^2 I_p \quad . \tag{2}$$

Equation (2) is based on the paraxial approximation of the wave equation, with the diffraction described by the operator $\exp(-iL/2k_0\nabla_\perp^2)$, where $\nabla_\perp^2=\partial^2/\partial x^2+\partial^2/\partial y^2$. The propagation length is L and K_0 is the wave number of the light.

Inserting Eq. (2) into Eq. (1), we end up with a single nonlinear partial differential equation. A linear stability analysis of this model [7], predicts a critical transverse wave number $k_c\sim\sqrt{L/k_0}$ to become unstable above the threshold, determining the typical pattern length scale. Far above the threshold, the single critical wave number broadens to a continuous band of active wave numbers.

Object of our analysis are the experimental spot patterns obtained for different values of the pump laser intensity I_p. If the system is not driven into saturation, just above threshold stationary patterns of hexagonally arranged bright spots develop. Under further increase of the pump laser intensity the spots begin to move, and the initial order breaks down. The pump intensities considered here range from a value just above the threshold of pattern formation $I_{th}^{(1)}$ to an eight times larger value of $I_{rel}\equiv I_p/I_{th}^{(1)}\leqslant 8$.

Up to this value, individual spots of approximately the same size are identifiable, which allows to reduce the continuous intensity distributions to the coordinates of a spatial arrangement of individual spots. Typical snapshots of experimental spot patterns are shown in Fig. 2. We define the locations of the spots as the centers of mass of islands of pixels exceeding a certain threshold value. For each fixed pump value, the spot positions of snapshots at ten different times have been determined. For the dynamic patterns, the period between two snapshots is chosen larger than the typical temporal correlation time. The following quantities obtained for a fixed pump value are averages over these ten realizations.

The number of spots is not a conserved quantity. Particularly in the dynamical, disordered regime, spots are frequently created and annihilated, as already described earlier for numerical simulations of a similar system [4]. As a first

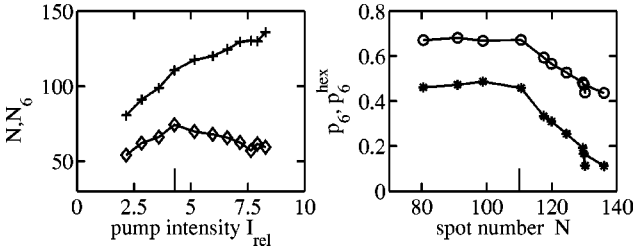

FIG. 3. Left: Average number of spots (+) and the number of six-sided Voronoi cells N_6 ($\diamond$) plotted vs the relative pump intensity I_{rel}. Right: Fraction p_6 of six-sided cells ($\bigcirc$), plotted against the corresponding average number of spots, together with p_6^{hex} (*), characterizing the presence of hexagonal domains.

measure, we have determined the average number of spots, N, for each fixed pump intensity I_{rel}. Figure 3 shows an almost monotonic increase of $N(I_{rel})$, reflecting an increase of the spot density since the constant cross section of the laser beam fixes the active area. Correspondingly, the typical spot distances decrease. Although the predictions of the linear stability analysis are questionable far above threshold, this change in the typical length scale is approximately within the broadening of the unstable wavenumber band.

For the geometrical analysis of the spot patterns, methods are needed which apply to systems with a finite number of objects in a spatially restricted region. One tool, well-known from the characterization of melting processes, is the calculation of pair and triple distribution functions. This has been applied previously to similar experimental patterns for a defocusing nonlinearity, yielding a threshold behavior from order to disorder [5]. As we will show here, deeper insight can be gained from the Voronoi construction [10] due to the diagnostic ability of the Voronoi cells for the local and global spatial arrangements of the spots. A Voronoi cell is assigned to each spot containing all points in the plane closer to the center of the generating spot than to any other spot center. The Voronoi construction has also found wide application in the characterization of the two-dimensional melting [2,3]. In these systems, the perfectly ordered structure is obtained at highest packing fraction, characterized by Voronoi cells which are regular hexagons. With increasing disorder, cells with smaller and larger numbers of edges (*defects*) appear, whereas the average number of sides of a cell is always six [10]. Hence, the construction of Voronoi tessellations allows to compare the degrees of order in the spot patterns with those from completely different pattern forming systems, as, e.g., the cellular structures in Bénard–Marangoni convections [11].

We have generated the Voronoi tessellations of the spot positions for each snapshot separately. In order to avoid boundary effects, cells at the boundary of the active area have not been taken into account. Parts of two typical Voronoi tessellations generated from experimental spot patterns are shown in Fig. 4. In the tessellation obtained for the lower relative pump intensity (a), large domains of hexagonally arranged spots can be detected. These domains shrink with increasing pump intensity (b) due to the generation of disordered regions with smaller cells. Typical arrangements of dislocations, as observed in crystals at the melting transition [2,3] or in the Bénard-Marangoni cellular structures [11], are hard to find in these tessellations in Fig. 4.

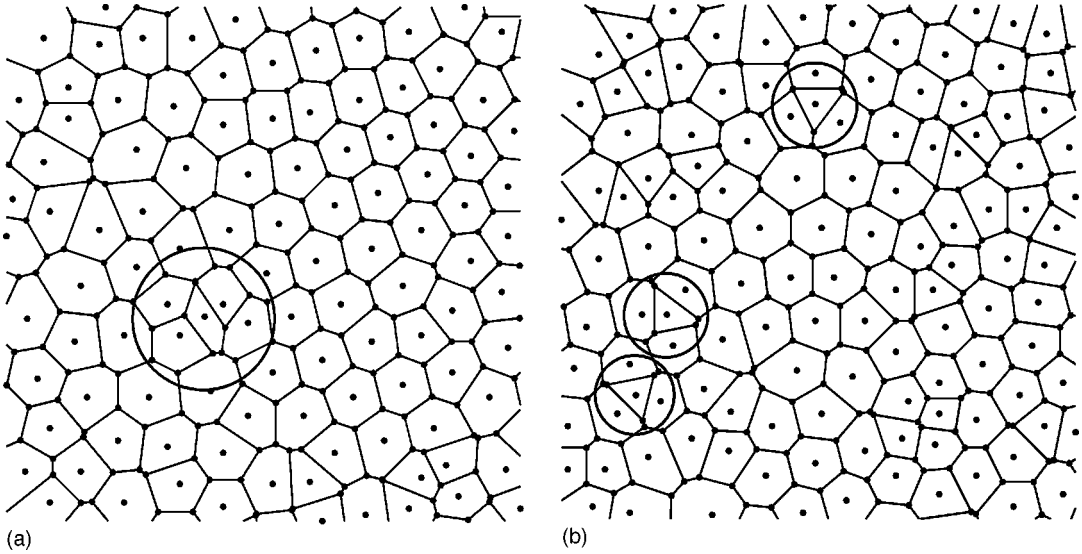

FIG. 4. Parts of the Voronoi tessellations generated by the spot positions of two snapshots, taken at relative pump intensities $I_{rel}=3.6$ (a) and $I_{rel}=5.16$ (b). The circles mark spots, appearing on the vertices of a local regular grid.

For the spot patterns, the calculated average number of six-sided cells, N_6, is represented in Fig. 3, left, as a function of the pump intensity. Perfect order is never achieved: $N_6 < N$ for all pump intensities. We assign the lack of perfect order even at low pump intensities to experimental imperfections like the presence of spatial inhomogeneities of the optical nonlinearity.

A commonly used measure of the degree of order is the relative frequency of six-sided cells, $p_6=N_6/N$. The picture becomes clearer, plotting its dependence on the average spot number (Fig. 3, right). For low pump intensities, the plateau of high values of p_6 is maintained under creation of new spots. At $N\approx 110$, however, the picture changes: the enhanced density yields a decrease of N_6 leading to a remarkable decay of p_6, showing evidence for a distinct threshold for the onset of disorder. The corresponding pump value of $I_{rel}\approx 4.3$ agrees with findings from entirely different approaches [7,8]. Our result differs completely from simple hard-core systems, which tend to order with increasing density.

Furthermore, the fraction of defects in the spot patterns, even at low pump intensities, is remarkably larger than in most other systems at the order-disorder transition [2,3,11]. For Voronoi tessellations of simple hard-disk systems e.g., [3], all values of p_6, obtained here, would correspond exclusively to the fluid phase which has a minimal value of $p_6^{RVT}=0.29$ for an uncorrelated gas at vanishing density.

Due to the relatively high fraction of defects, it is not clear how much the six-sided cells are gathered in domains with locally high hexagonal order, i.e., whether p_6 is still a reliable measure for the degree of spatial order. A simple estimate of the fraction of spots arranged in hexagonally ordered domains can be performed by the measurement of the relative frequency of six-sided cells, surrounded by at least four six–sided cells, p_6^{hex}. The quantitative behavior of p_6^{hex}, represented in the right-hand panel of Fig. 3, clearly shows that the decrease of p_6 is caused by the decrease of p_6^{hex} and thus is in fact a consequence of the breakdown of hexagonal domains. We conclude that a regular hexagon pattern can bear only a certain number of (additional) spots. Above a critical value of the spot density, this spatial order breaks down.

In order to gain a better understanding of the unusual density dependence of the breakdown of order in the spot patterns, the metrical properties of the cells are considered now. One great advantage of the Voronoi construction is that it enables us to distinguish spots in locally ordered from those in disordered regions. Whereas the distribution of areas of the Voronoi cells yields no further significant information (not shown here), additional information can be gained from the statistics of the areas of the cells' largest inscribed circles, centered at the spot positions. The circle area A_c is simply related to the nearest–neighbor distance d: $A_c=\pi(d/2)^2$. In an ordered system, the distribution of circle areas exhibits a narrow peak, whereas for a random distribution of points, it decays exponentially. In Fig. 5, the histograms of the circle areas A_c are shown for three different relative pump intensities. We have distinguished the contributions from cells belonging to hexagonal domains - as defined above (black bars) and those from all other cells (white bars).

At a relative pump intensity $I_{rel}=3.6$, when p_6 has its maximum value, $N(A_c)$ exhibits a strong peak at large values of $A_c\approx 40$ a.u., dominated by the cells from ordered hexagonal domains. Just above the critical pump intensity at

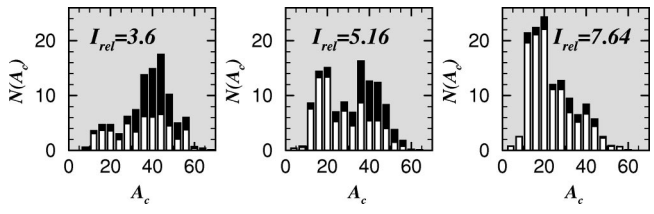

FIG. 5. Average number of cells with circle area A_c (in arbitrary units). Black bars represent the contribution from hexagons with at least four six-sided neighbors. White bars represent the contributions from all other cells.

$I_{rel}=5.16$, a distinct second peak at much smaller areas $A_c \approx 20$ a.u. builds up, and the distribution becomes bimodal: coinciding with the breakdown of order, we observe the appearance of a new type of spots with small nearest–neighbor distances. In the disordered regime, at $I_{rel}=7.64$, the right peak in $N(A_c)$ as well as the hexagonal domains have disappeared almost completely, whereas for small circle areas, $N(A_c)$ shows a strongly enhanced weight. This result also indicates the existence of a distinct minimum distance between spots. Remarkably smaller nearest-neighbor distances with increasing disorder have also been reported for the topological defect structures in a chemical reaction-diffusion system at the transition from rotating spirals to spatio–temporal chaos [12].

Our results lead to the conjecture that in the experimental case with increasing density, spots are preferably created between hexagonally ordered spots. This mechanism would explain the coincidence of the breakdown of hexagonal domains and the strongly enhanced weight at smaller nearest-neighbor distances. In fact, typical examples of spots appearing on vertices of quite regular tessellations or at dislocations of the hexagonal grid can be detected in the Voronoi diagrams represented in Fig. 4. We have marked these cells by large circles centered at the positions of the additional spots. The shape of these cells appears triangular, their area simply seems to cut parts of the three neighboring cells.

The competition of two physical mechanisms, which govern the formation of the spot patterns, may explain our observations. On one hand, the Talbot effect describes the exact repetition of a spatially periodic wave front after a certain propagation length. This happens, while the light wave in the feedback system propagates from the LCLV read-out to its write side, supporting the evolution of well ordered, periodic patterns [9]. On the other hand, a single spot can be created by a self-focusing effect. A bright spot belongs to a peak in the induced phase $\Phi(x,y)$, representing a small induced lens. This lens focuses the pump light onto its position on the LCLV write side, such in turn supporting the phase peak. The latter can in principle happen, wherever enough pump intensity is supplied, i.e., also between spots of an existing hexagonal pattern. Consequently, self-focusing will become more dominant with increasing pump intensity. Also, this local effect is probably promoted by spatial inhomogeneities. A competition appears, since the Talbot effect disfavors such deviations from an ideal periodic pattern.

The relation between spatial order and dynamics so far is not clear. One possibility would be that when newly formed spots cannot be integrated into a regular pattern, the interacting spots will not come to rest. They keep moving, trying to keep their mutual minimal distance.

To conclude, the clearly detectable breakdown of order in optical spot patterns neither resembles a melting process nor the order-disorder transition in Bénard-Marangoni structures. Making use of an extension of the classical Voronoi analysis, we find strong evidence that the creation of spots between spots in originally ordered regions in combination with the irregular motion destroys the order.

The experiments were performed by Bernd Thüring at the Institute of Applied Physics at the Darmstadt University of Technology. R.N. would like to thank M. Bär for his support and the Max-Planck-Gesellschaft for the opportunity to work at the MPI-PKS in Dresden.

[1] M. C. Cross and D. Hohenberg, Rev. Mod. Phys. **65**, 851 (1993); P. Manneville, *Dissipative Structures and Weak Turbulence* (Academic Press, San Diego, 1990).

[2] F. H. Stillinger and T. A. Weber, J. Chem. Phys. **74**, 4015 (1981); T. A. Weber and F. H. Stillinger, *ibid.* **74**, 4020 (1981); K. J. Strandburg, Rev. Mod. Phys. **60**, 161 (1988); J. F. Fernandez, J. J. Alonso, and J. Stankiewicz, Phys. Rev. E **55**, 750 (1997).

[3] J. Lemaître, J. P. Troadec, A. Gervois, and D. Bideau, Europhys. Lett. **14**, 77 (1991); J. Lemaître, A. Gervois, J. P. Troadec, N. Rivier, M. Ammi, L. Oger, and D. Bideau, Philos. Mag. B **67**, 347 (1993).

[4] G. D'Alessandro and W. J. Firth, Phys. Rev. A **46**, 537 (1992).

[5] B. Thuering, R. Neubecker, and T. Tschudi, Opt. Commun. **102**, 111 (1993); R. Neubecker, B. Thüring, M. Kreuzer, and T. Tschudi, Chaos, Solitons and Fractals **4**, 1307 (1995).

[6] S. A. Akhmanov, M. A. Vorontsov, and V. Yu. Ivanov, Pis'ma Zh. Éksp. Teor. Fiz. **47**, 611 (1988) [JETP Lett. **47**, 707 (1988)]; E. Pampaloni, P. -L. Ramazza, S. Residori, and F. T. Arecchi, Europhys. Lett. **24**, 647 (1993); F. T. Arecchi, A. V. Larichev, and M. A. Vorontsov, Opt. Commun. **105**, 297 (1994).

[7] R. Neubecker, G. -L. Oppo, B. Thuering, T. Tschudi, Phys. Rev. A **52**, 791 (1995); B. Thüring, R. Neubecker, M. Kreuzer, E. Benkler, and T. Tschudi, Asian J. Phys. **7(3)**, 453 (1998).

[8] R. Neubecker, B. Thüring, M. Kreuzer, and T. Tschudi, Chaos, Solitons and Fractals **10(4-5)**, 681 (1999); R. Neubecker, B. Thüring, and T. Tschudi (unpublished).

[9] E. Ciaramella, M. Tamburrini, E. Santamato, Appl. Phys. Lett. **63**, 1604 (1993).

[10] A. Okabe, B. Boots, and K. Sughihara, *Spatial Tessellations* (Wiley, New York, 1995).

[11] R. Ocelli, E. Guazelli, and J. Pantaloni, J. Phys. (France) Lett. **44**, 567 (1983); P. Cerisier, S. Rahal, and N. Rivier, Phys. Rev. E **54**, 5086 (1996).

[12] M. Hildebrand, M. Bär, and M. Eiswirth, Phys. Rev. Lett. **75**, 1503 (1995).